MECH 309

Murman-Cole Scheme for the Transonic Small Disturbance Equation

Khaled Al Masaid 260623070

Chris Jing 260634735

Pierrick Hamard 260619897

Ahmed Zedan 260662619

December 4th, 2019

Dept. of Mechanical Engineering

McGill University

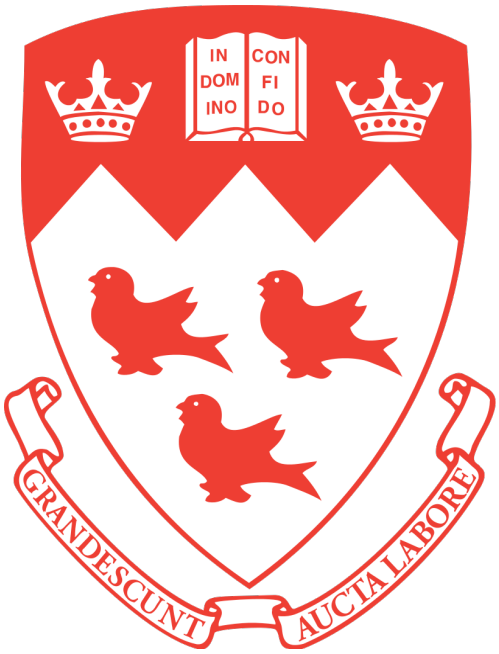

Presented to:

Prof. Siva Nadarjah

Summary

1 Problem Definition **3**

1.1 Transonic Small Disturbance Equation . . . 3

1.2 Boundary Conditions . . . 3

1.3 Tangency Boundary Condition . . . 4

2 Murman-Cole Method **5**

2.1 Pseudo-code . . . 6

2.1.1 Jacobi Method . . . 6

2.1.2 Coefficient of Pressure . . . 6

3 Results **6**

4 Results for Jacobi with a Coarse Grid ($\Delta x = \Delta y = 0.1$) **7**

4.1 L_∞-norm convergence plots . . . 7

4.2 $C_p(x)$ along airfoil using grid size $\Delta x = \Delta y = 0.1$ . . . 7

4.3 Pressure Contours . . . 8

4.3.1 M=0.75 . . . 9

4.3.2 M=0.77 . . . 9

4.3.3 M=0.79 . . . 10

4.3.4 M=0.81 . . . 10

4.3.5 M=0.83 . . . 11

4.3.6 M=0.85 . . . 11

5 The Effects of Grid Spacing **12**

6 $C_p(x)$ Along Airfoil Over Range of M_{inf} for a Fine Grid **12**

7 Conclusion **13**

List of Figures

1 Applied Boundary Conditions . . . 4

2 Computational grid . . . 5

3 Convergence plot of the L_∞-norm . . . 7

4 Surface pressure coefficient as a function of x . . . 8

5 Pressure contour for M=0.75 . . . 9

6 Pressure contour for M=0.77 . . . 9

7 Pressure contour for M=0.79 . . . 10

8 Pressure contour for M=0.81 . . . 10

9 Pressure contour for M=0.83 . . . 11

10 Pressure contour for M=0.85 . . . 11

11 C_p over airfoil surface for a range of grid sizes . . . 12

12 C_p over airfoil surface for fine grid size . . . 13

1 Problem Definition

Numerical solutions of the transonic small-disturbance (TSD) equation can be computed using the Murman-Cole method. Transonic flows have a mach number range $0.8 < M < 1.2$ and often occur in compressible flows. For the purpose of this project the flow over a circular arc airfoil will be studied. In 1971, Murman and Cole developed a method that replaced the TSD equation with finite difference formulas for the derivatives and successfully solved the TSD equation 1. The resulting system of non-linear equations can be solved using iterative methods including Jacobi, Gauss-Seidel or Successive over-relaxation.

1.1 Transonic Small Disturbance Equation

The flow is assumed to be primarily in the x-direction parallel to the airfoil chord (i.e. $\frac{\partial \phi}{\partial y} = v \approx 0$). The governing equation is the two-dimensional TSD equation given by:

$$\left[(1 - M_\infty^2) - (\gamma + 1) M_\infty^2 \frac{\phi_x}{U_\infty}\right] \phi_{xx} + \phi_{yy} = 0 \tag{1}$$

where M_∞ is the free-stream Mach number, $\gamma = 1.4$ is the specific heat ratio of air, ϕ is the velocity potential. The Murman-Cole method will be used to write equation 1 above into a difference equation setup over a rectilinear grid (i,j). The airfoil will be located on the grid line $i = const.$ parallel to the x-axis. The airfoil chord has unity for length. The leading edge is located at $x = 20$ and trailing edge at $x = 21$.

1.2 Boundary Conditions

In order to compute the transonic flow over an airfoil, the following boundary conditions are applied on the airfoil's upper and lower surfaces. The airfoil boundary conditions are embedded into the difference formulas at points inside the grid that has constant spacing in the x and y directions over the airfoil. Figure 1 below illustrates the boundary conditions applied on the rectilinear grid.

1. $\phi(x, y) = 0 \quad \forall$ (0,y), (50,y) $\in 0 \leq y \leq 50$; (x,50) $\in 0 \leq x \leq 50$
2. $\frac{\partial \phi}{\partial n} = 0 \quad \forall\ (x, 0) \notin 20 \leq x \leq 21$
3. $\frac{\partial \phi}{\partial n} = U_\infty \frac{dy}{dx} \quad \forall\ (x, 0) \in 20 \leq x \leq 21$

$\frac{\partial \phi}{\partial n}$ is equal to zero everywhere except on the airfoil surface. The gas constant R for air is $R = 287.058\ Jkg^{-1}k^{-1}$, free-stream static temperature and pressure are $T_\infty = 293$ K and $P_\infty = 100\ kN/m^2$ respectively and (x,y) $\in [0, 50]^2$ spans the two-dimensional domain. The circular-arc airfoil is defined by the following equation:

$$y(x) = (t/c)(-2x^2 + 82x - 840) \quad \forall\ (x, 0) \in 20 \leq x \leq 21$$

where $t/c = 0.08$ is the thickness ratio.

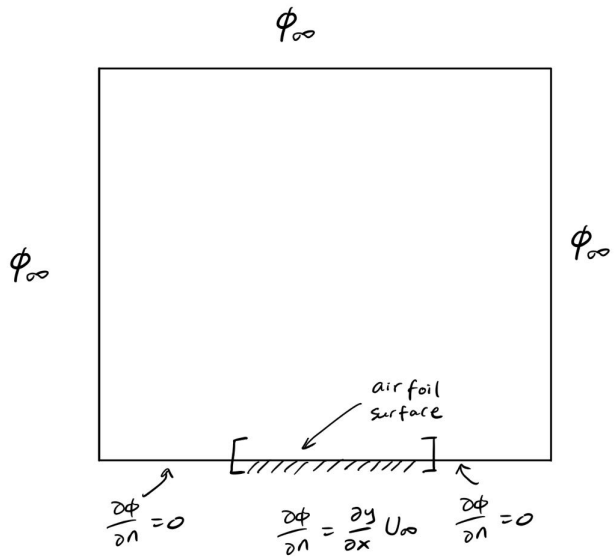

Figure 1: Applied Boundary Conditions

1.3 Tangency Boundary Condition

The tangency boundary conditions along the surface of the airfoil needs to be satisfied. The flow is tangent to the surface where $\vec{V} \cdot \vec{n} = 0$.

The following can be obtained:

$$\tan\theta = \frac{v'}{U_\infty + u'}$$

If $\theta << 1$, then:

$$\tan\theta \approx \frac{v'}{U_\infty} \approx \frac{dy}{dx}$$

By definition,

$$v' = \phi_y$$

$$\phi_y = \phi_n$$

Finally we can get,

$$\frac{\partial\phi}{\partial n} = U_\infty \frac{dy}{dx}$$

$$\frac{\phi_{i,2} - \phi_{i,1}}{\Delta y} = U_\infty \frac{dy}{dx}$$

2 Murman-Cole Method

The basic idea behind the Murman-Cole method is to replace a PDE with finite difference formulas for the derivatives. The discrete finite difference formulas divide an area into points of interest and allow to solve for every point using differentiation. A rectilinear grid of the flowfield is created as shown in figure 2 below:

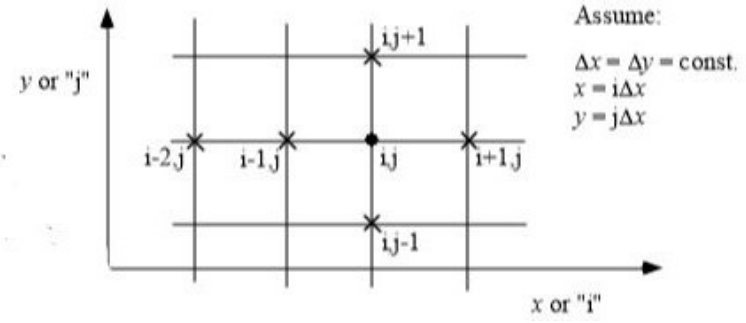

Figure 2: Computational grid

Starting with equation 1 we have:

$$A = \left[(1 - M_\infty^2) - (\gamma + 1)M_\infty^2 \frac{\phi_x}{U_\infty}\right]$$

Then:

$$A\phi_{xx} + \phi_{yy} = 0$$

If A_{ij} is > 0 then the flow is locally subsonic and it is an elliptic PDE. For a subsonic region we use a centered difference scheme for ϕ_{xx} and ϕ_{yy} and we get:

$$A\delta_x^2\phi_{ij} + \delta_y^2\phi_{ij} = 0$$

If A_{ij} is < 0 then the flow is locally supersonic and the problem becomes a hyperbolic PDE and we get:

$$A_{i-1,j}\delta_x^2\phi_{i-1,j} + \delta_y^2\phi_{ij} = 0$$

For both the subsonic and supersonic cases, the following formula for A_{ij} will be used:

$$A_{ij} = (1 - M_\infty^2) - (\gamma + 1)\frac{M_\infty^2}{U_\infty}\frac{\phi_{i+1,j} - \phi_{i-1,j}}{2\Delta x}$$

Based on the value of A_{ij}, four different scenarios can be combined into a single difference equation that is discontinuous. Equation 2 below corresponds to the solution of the PDE.

$$\mu_{ij} = \begin{cases} 0 & \text{if } A_{ij} > 0 \\ 1 & \text{if } A_{ij} < 0 \end{cases} \tag{2}$$

The Murman-Cole method can then be expanded and written as the PDE shown in the equation below:

$$\frac{(1-\mu_{ij})A_{ij}}{(\Delta x)^2}\phi_{i+1,j} + \left[\frac{\mu_{i-1,j}A_{i-1,j}}{(\Delta x)^2} - \frac{2(1-\mu_{ij})A_{ij}}{(\Delta x)^2} - \frac{2}{(\Delta y)^2}\right]\phi_{ij} + \frac{1}{(\Delta y)^2}\phi_{i,j+1}$$
$$+ \left[\frac{(1-\mu_{ij})A_{ij}}{(\Delta x)^2} - \frac{2\mu_{i-1,i}A_{i-1,j}}{(\Delta x)^2}\right]\phi_{i-1,j} + \left[\frac{\mu_{i-1,j}A_{i-1,j}}{(\Delta x)^2}\right]\phi_{i-2,j} + \frac{1}{(\Delta y)^2}\phi_{i,j-1} = 0$$

This method can be solved using Gauss-Seidel, Jacobi or SOR using an equally spaced grid.

2.1 Pseudo-code

We begin by initializing the flow by setting $\phi = 0$ everywhere to simplify the computation and lower the time cost. The boundary conditions on the lower wall are then imposed and satisfied as mentioned earlier. The variable ϕ_{ij} needs to be updated $\forall\ i = 3; \quad i_{max} - 1$ and $\forall\ j = 2, \quad j_{max} - 1$ (along bottom surface) at every iteration.

2.1.1 Jacobi Method

For the purposes of this project the Jacobi iterative method will be used in the following form:

$$c_{ij}^k \phi_{i,j-1}^k + g_{ij}^k \phi_{i-2,j} + d_{ij}^k \phi_{i-1,j}^k + a_{ij}^k \hat{\phi}_{i,j}^{k+1} + e_{ij}^k \phi_{i+1,j}^k + b_{ij}^k \phi_{i,j+1} = 0$$

The equation can be re-arranged in terms of $\hat{\phi}_{i,j}^{k+1}$ and give the following:

$$\hat{\phi}_{i,j}^{k+1} = \frac{-c_{ij}^k \phi_{i,j-1}^k - g_{ij}^k \phi_{i-2,j}^k - d_{ij}^k \phi_{i-1,j}^k - e_{ij}^k \phi_{i+1,j}^k - b_{ij}^k \phi_{i,j+1}}{a_{ij}^k}$$

This is the final iterative scheme used to update all the internal values of $\phi_{i,j}$ every iteration

2.1.2 Coefficient of Pressure

Determining the pressure distribution along the surface of the airfoil is essential. The coefficient of pressure (C_p) is an important parameter for studying the flow over airfoils. C_p describes the relative pressure at a point within a flow field. In general, it varies at every point in the fluid flow. C_p can be evaluated at critical points around the airfoil that can be used to determine the pressure at that location which is essential for engineering applications. The position of a shock can be determined by the location of the largest gradient of the surface pressure distribution [ref.2]. The coefficient of pressure is dimensionless, it can be computed through the pressure distribution along the surface of the airfoil and, in our case, is given by:

$$C_p \approx \frac{-2\phi_x}{U_\infty}$$

which we can approximate using a central difference formula for ϕ_x:

$$C_p \approx \frac{-2}{U_\infty} \frac{\phi_{i+1,j} - \phi_{i-1,j}}{2\Delta x} = -\frac{\phi_{i+1,j} - \phi_{i-1,j}}{U_\infty \Delta x}$$

3 Results

The Jacobi iterative method was used to solve the TSD equation. This part of the report was used to setup the spacing of the computational grid, initialize matrices and build different plots for varying mach numbers. The associated MATLAB script is attached with this project. Based on the Jacobi method, we created a function to compute ϕ in the computational domain given a set grid spacing (Δx), free stream mach number (M_{inf}), maximum error for convergence ($tol = 1e-04$), and total grid size (i.e. $(x, y) \in [0, max_{bnd}]^2$ where maxbnd = 50 in all cases in this project).

```
[phi, error, c_p, P, iteration] = TSD_Solve(dx, M_inf, tol, max_bnd)
```

Our function then returns the converged *phi* matrix, the error for each iteration (L_∞ norm), the pressure coefficient matrix, the pressure ratio ($\frac{P}{P_\infty}$) matrix, and total number of iterations.

4 Results for Jacobi with a Coarse Grid ($\Delta x = \Delta y = 0.1$)

The following plots were obtained for Mach numbers in the range [0.75,0.85] with 0.02 increments.

4.1 L_∞-norm convergence plots

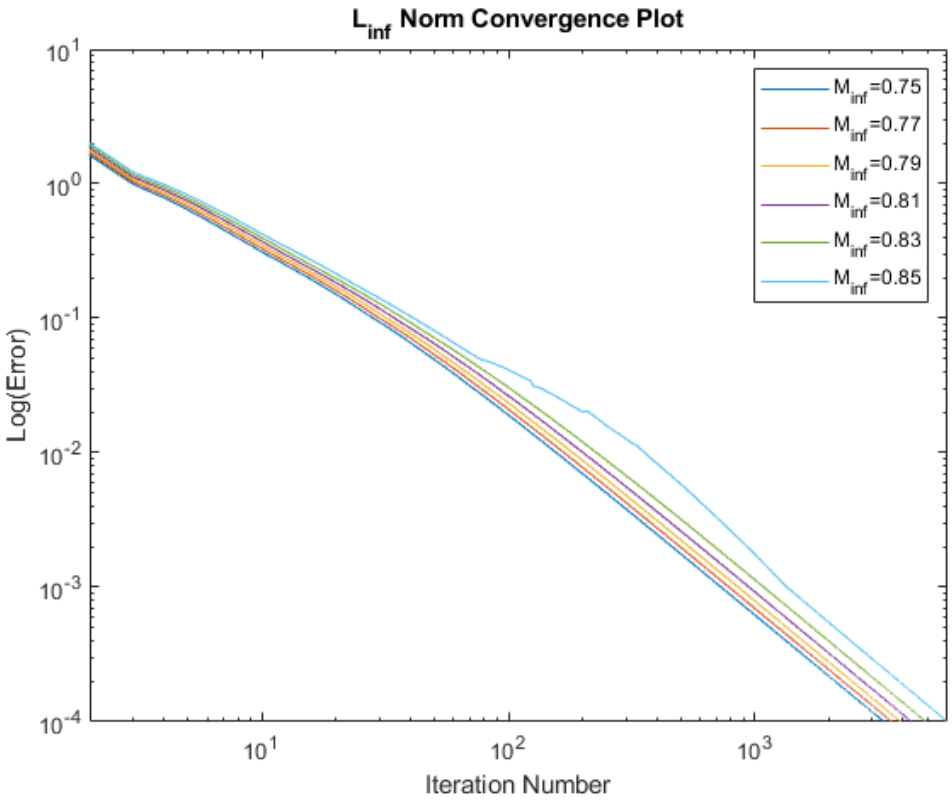

Figure 3: Convergence plot of the L_∞-norm

The curves for the different Mach numbers were plotted on one graph as shown above in figure 3. The plot shows as the mach number increases, the number of iterations required increases and that is due to the complexity of region where pressure is high and shocks can occur. The solutions shown above ranged in iterations from about 3300 to 5900 at the largest value for M_{inf}

4.2 $C_p(x)$ along airfoil using grid size $\Delta x = \Delta y = 0.1$

Figure 4 shows the change in pressure coefficient as the flow passes over the airfoil. The graph shows that $C_p(x)$ is greater in magnitude for higher mach numbers at the same point. For mach numbers < 0.83, no shocks are present and the curves are almost parabolic. For mach numbers ≥ 0.83, a shock wave begins to appear and as M increases, the shock start to shift towards the trailing edge of the airfoil.

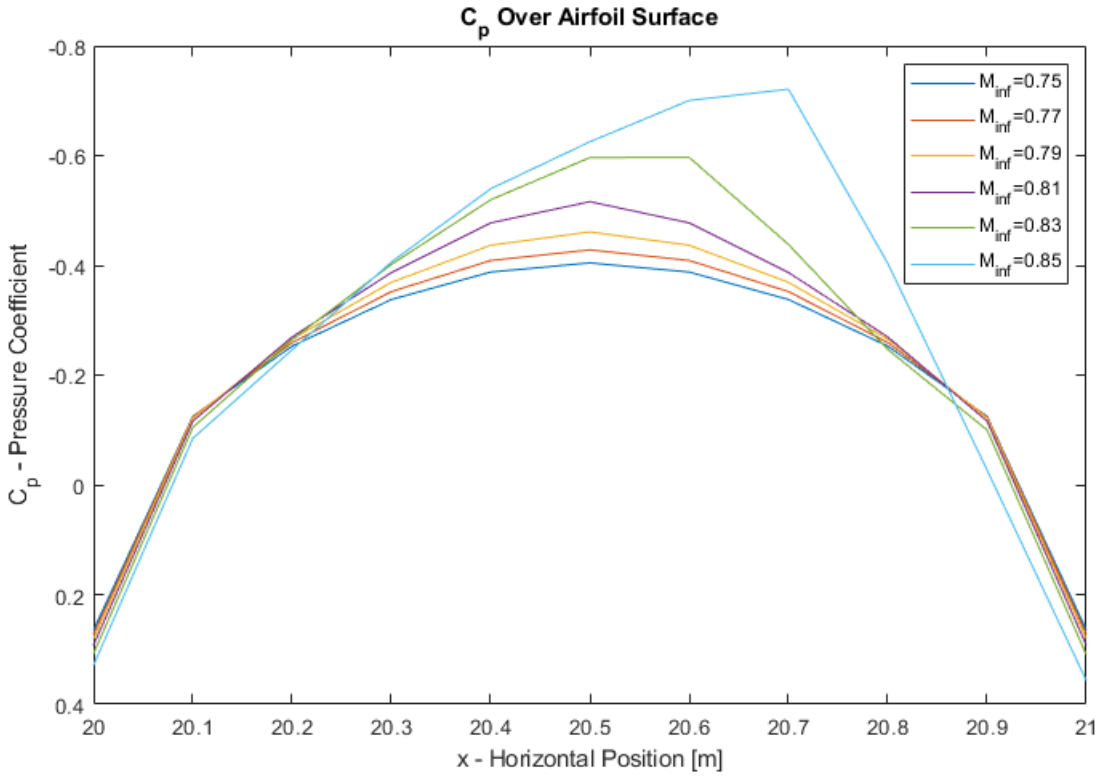

Figure 4: Surface pressure coefficient as a function of x

4.3 Pressure Contours

The following contour plots were created for the different mach numbers. The plots model the three-dimensional airfoil model on a two-dimensional plane for $x \epsilon [20, 21]$ and $y \epsilon [0, 1]$. The plots display the $\frac{P}{P_\infty}$ ratio in the square region that lies directly on the airfoil surface. As the mach number increases, the curves become less refined with the curve changing from smooth parabola-type to a combination of straight lines around the mid-point ($x = 20.5$) region. As illustrated in figures 5 to 8 below, the flow has an even distribution over the airfoil and no shocks are observed. The color bar indicates the values of $\frac{P}{P_\infty}$. As $\frac{P}{P_\infty}$ increases, the local pressure increases and therefore pressure is higher further away from the airfoil. Flows with mach numbers ≥ 0.83 have shocks present as illustrated in figures 9 and 10. As the free-stream mach number increases, the shock moves from near the center chord ($x = 20.5$) towards the trailing edge. It is also observed that for higher mach numbers there is a larger drop in pressure after the shock, indicating a stronger shock. All graphs indicate very high pressure points near the leading edge ($x = 20.1$) and trailing edge ($x = 20.9$) illustrated by the yellow color.

4.3.1 M=0.75

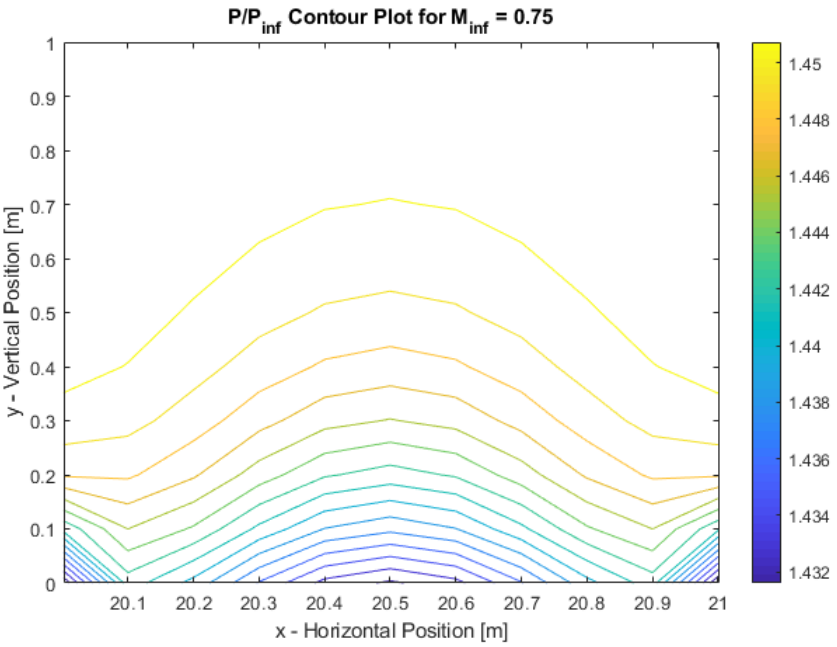

Figure 5: Pressure contour for M=0.75

4.3.2 M=0.77

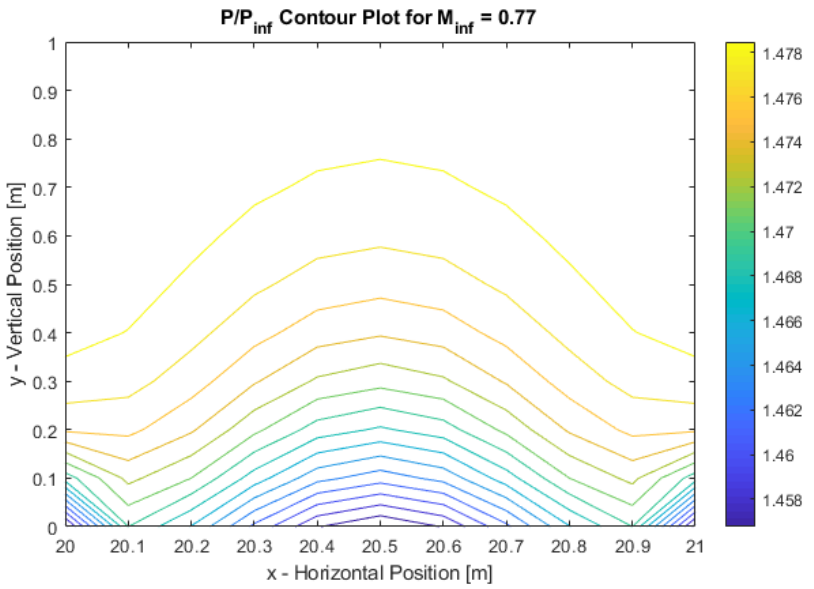

Figure 6: Pressure contour for M=0.77

4.3.3 M=0.79

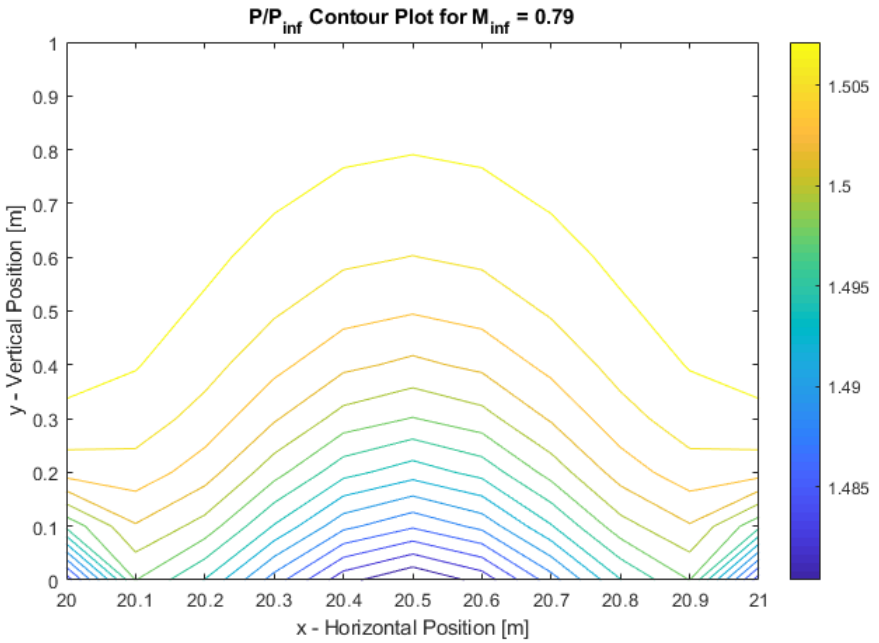

Figure 7: Pressure contour for M=0.79

4.3.4 M=0.81

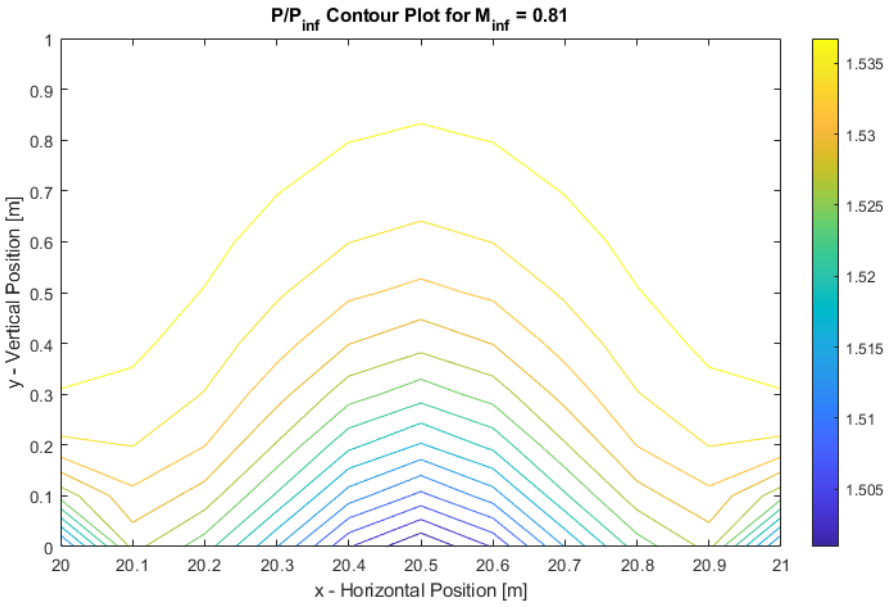

Figure 8: Pressure contour for M=0.81

4.3.5 M=0.83

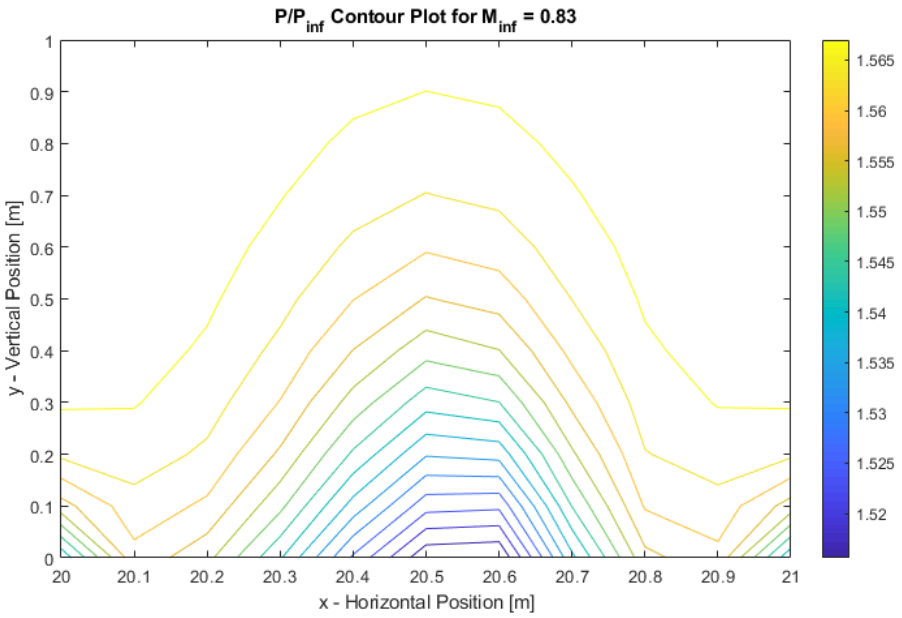

Figure 9: Pressure contour for M=0.83

4.3.6 M=0.85

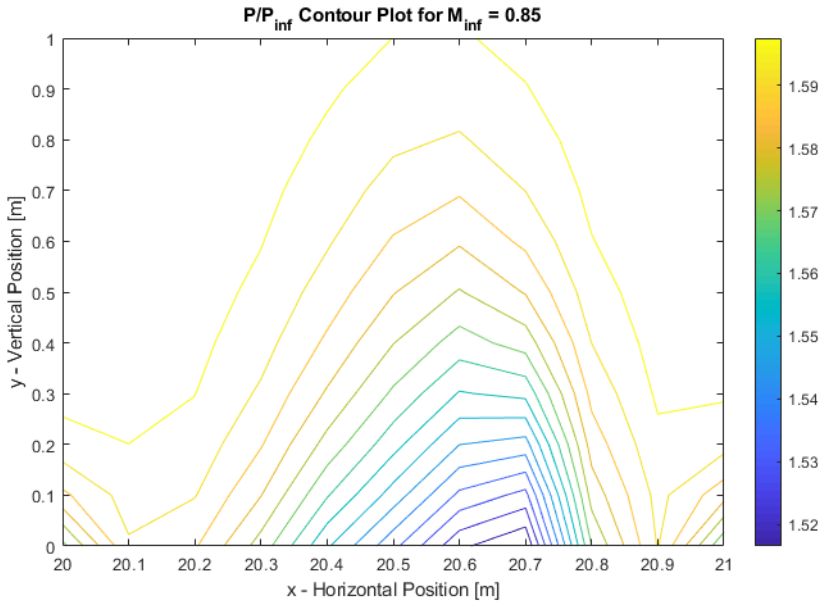

Figure 10: Pressure contour for M=0.85

5 The Effects of Grid Spacing

Three different grid sizes were created. The course grid has constant spacing $\Delta x = \Delta y = 0.1$, medium grid $\Delta x = \Delta y = 0.05$ and fine grid $\Delta x = \Delta y = 0.025$. The effect of decreasing gird size is illustrated in figure 11 below. The graph displays the curves of pressure coefficient C_p for the different grids at M=0.83. The fine grid had the smallest spacing, and as as a result, the curve is smoother and more defined. It can also be seen that for a change in grid size, the shock wave location (which occurs roughly at $x = 20.6m$) does not change. However, with increasing grid size, the behavior of the shock is better defined as the curve is sharper where rapid pressure drop occurs.

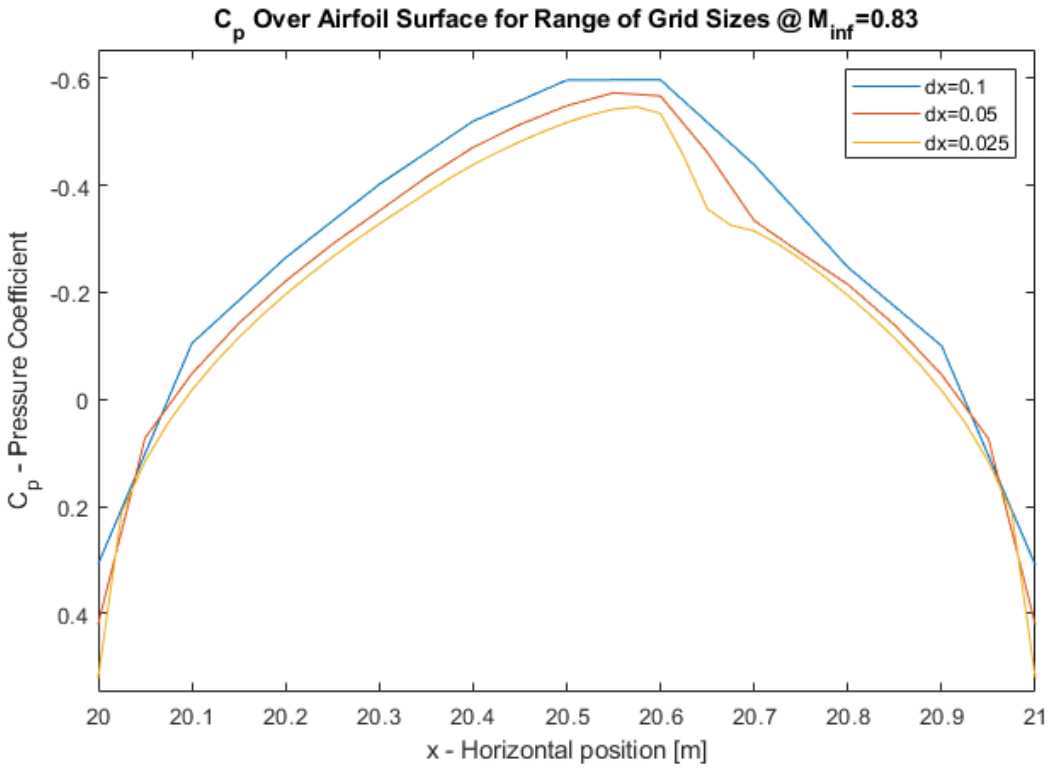

Figure 11: C_p over airfoil surface for a range of grid sizes

6 $C_p(x)$ Along Airfoil Over Range of M_{inf} for a Fine Grid

As discussed earlier, the curves are more defined for the smaller spacing in a finer mesh. Figure 12 below displays pressure coefficient over the airfoil for a range of mach numbers between [0.75, 0.85] at intervals of 0.02 using a fine grid spacing ($\Delta x = \Delta y = 0.025$). When comparing this result to the coarse grid size (Fig. 4), it is clear that the curves are smoother and more detail is seen in the change of C_p through the shock.

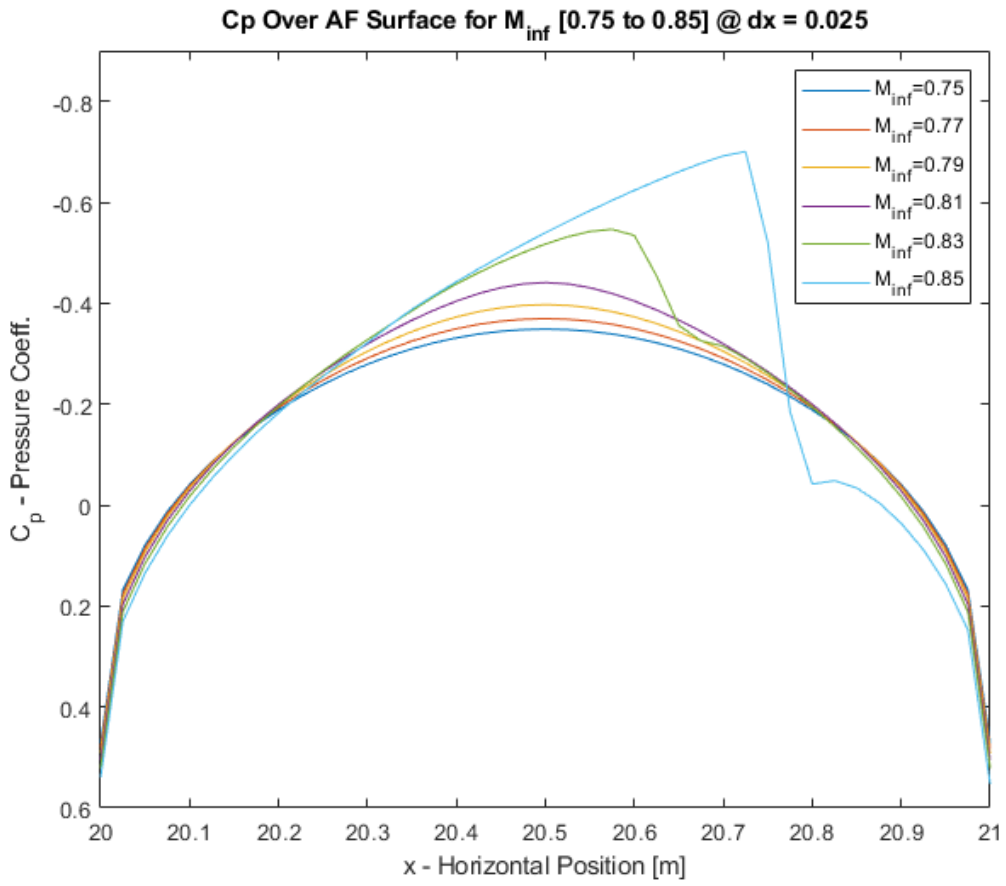

Figure 12: C_p over airfoil surface for fine grid size

7 Conclusion

In conclusion, numerical iterative methods can be used to accurately solve the transonic small-disturbance equation. The Murman-Cole method replaces the TSD equation with finite difference formulas. The resulting system of non-linear equations can be solved using iterative methods including: Jacobi, Gauss-Seidel or Successive over-relaxation, which for the case of this study, Jacobi was used. For increasing free stream mach numbers, the coefficient of pressure, and subsequently pressure, increases over the surface of the airfoil for $M_{inf} \geq 0.83$. In addition to this, the shock position occurs further downstream on the airfoil. Another interesting observation that can be made is that for increasing grid sizes, the shock position does not change but becomes more defined. For future studies it would therefore be beneficial to use finer grid sizes for greater accuracy of results.